Hindawi
Mobile Information Systems
Volume 2019, Article ID 7547431, 12 pages
https://doi.org/10.1155/2019/7547431

Research Article

System Performance of Cooperative NOMA with Full-Duplex Relay over Nakagami-*m* Fading Channels

Xuan-Xinh Nguyen[1] **and Dinh-Thuan Do**[2]

[1]*Bach Khoa University, Ho Chi Minh City, Vietnam*
[2]*Wireless Communications Research Group, Faculty of Electrical and Electronics Engineering, Ton Duc Thang University, Ho Chi Minh City, Vietnam*

Correspondence should be addressed to Dinh-Thuan Do; dodinhthuan@tdtu.edu.vn

Received 10 October 2018; Revised 13 January 2019; Accepted 17 January 2019; Published 17 March 2019

Academic Editor: Mari C. Aguayo Torres

In this paper, we consider a dual-user nonorthogonal multiple access (NOMA) with the help of full-duplex decode-and-forward (DF) relay systems with respect to Nakagami-*m* fading channel environment. Especially, we derive the analytical expressions to evaluate system performance in terms of outage probability, achievable throughput, and energy efficiency. The main investigation is on considering how the fading parameters and transmitting power at the base station make crucial impacts on system performance in the various scenarios. Finally, simulations are conducted to confirm the validity of the analysis and show the system performance of NOMA under different fading parameters of Nakagami-*m* fading channels.

1. Introduction

With the fast growth related to cellular networks and WiFi network-aware transmission techniques, several wireless facilities to support smart devices are becoming more widespread trend. Massive connections and huge multimedia streaming are adapted to satisfy an explosive growth in the wireless data traffic transmission. As a widely recognized key technology for the fifth-generation (5G) mobile communication systems, nonorthogonal multiple access (NOMA) paradigm is proposed to support the tremendous demands on data traffic. NOMA recently investigated and the related novel architectures for NOMA have drawn great considerations in both academy and industry [1–3]. In the conventional orthogonal multiple access (OMA) schemes, in which at signal domains (i.e., frequency, time, or space), the different orthogonal channels are allocated for accommodated users. In contrast, NOMA assigns the same channel for such users. More specifically, different power levels are nominated to different data flows with assistance of the superposition coding (SC) at the transmitter. At the receiver, the successive interference cancellation (SIC) is deployed to detach separated signals. As a result, main advantages including massive connections, reduced communication latency, and increased spectral efficiency can be achieved by the deployment of NOMA [1, 2].

More recent works have considered the integration of cooperative relaying transmission with energy harvesting in systems [4–8] and with NOMA systems in [9–11]. The crucial advantage of the combined model is that users need the help of the dedicated relays cooperative in NOMA systems to further expand both transmission reliability and energy efficiency [12–20]. Specifically, users with strong channel conditions proceeded as relays to assist the users with weak channel conditions in a cooperative NOMA (C-NOMA) scheme proposed in NOMA-based cellular network [10]. Other trends are applications for wireless power transfer to NOMA as interesting investigation in [6, 8]; that is, simultaneous wireless information and power transfer (SWIPT) technique was used in relaying systems, in which trade-offs between outage performance and energy harvesting coefficients are examined. Additionally, the overlay cognitive radio (CR) networks can require C-NOMA, where a secondary transmitter [12] or a secondary receiver [13]

helps as a relay and supports transmitting the primary messages, and hence, the primary network assigned the same frequency band can be able to deliver multiple access capabilities. To expand the performance, a dedicated relay can be employed in NOMA systems [14–20]. In [14, 15], the classical three-node cooperative relaying system (CRS) was applied in NOMA, where the source transfers two symbols with dissimilar power levels possessing superposition coding to a dedicated half-duplex relay so that the acquired symbols corresponding to two time slots are forwarded to the destination. In [16, 17], to increase the performance of the user with the poor channel condition, two-user NOMA systems were measured in two scenarios, including deploying a dedicated half-duplex relay [16] and deploying a dedicated full-duplex relay [17]. Additionally, a variable gain relay was presented to simplify the transmission between the source and NOMA users to serve multiusers in NOMA systems in the case of nonexistence of direct link transmissions as in [18]. System performance such as exact and asymptotic high signal-to-noise ratio (SNR) expressions were presented to illustrate the superiority of NOMA over orthogonal multiple access (OMA) with respect to applied Nakagami-m fading channels [20]. While a fixed gain relay and direct link transmissions were considered to examine performance in concerned NOMA-based relaying networks [18, 19]. With regard to wireless power transfer, a SWIPT-based decode-and-forward (DF) relay was considered in NOMA-based relaying network [21].

Recently, due to its potential to double the spectral efficiency, full-duplex (FD) wireless communication has attracted substantial attentions by permitting concurrent downlink (DL) and uplink (UL) transmission in the same frequency band [22–24]. The two-way communication links in a two-user FD scheme were inspected in terms of the rate region and the achievable sum rate [25, 26], respectively. Most of the researches on NOMA schemes rely on the Rayleigh fading channel model. Nevertheless, Rayleigh fading is considered as the special case of fading channels. Alternately, it is the most effective way to consider influences of Nakagami-m fading channels in the outage performance evaluation of NOMA with regard to the line of sight (LoS) transmission. To our best knowledge, the wide-ranging topic-related wireless analysis, i.e., Nakagami-m fading channels in relaying-aware NOMA, has not been well considered yet in the previous literature. In [18], the closed form and lower and upper bounds on the ergodic sum rate together with the outage probability have been provided in amplify-and-forward (AF) relaying over Nakagami-m fading channels, whereas the achievable rates over Rayleigh fading channels in the decode-and-forward (DF) scheme have been explored in [27]. Contrasting with the case single of antenna equipped in all nodes as recent works [18, 27], the outage performance analysis over Rayleigh fading channels deploying multiple antennas has been assigned for the source and all destinations in [28]. Furthermore, by resolving the combined power allocation and relay beamforming scheme, the maximum sum rate has been attained in the case of multiple antennas equipped in the relay, while the single antenna is equipped in source and all destinations [29]. In [30], the authors studied the performance of the cooperative relay scheme with a single relay over Nakagami-m fading channels in terms of downlink in NOMA, in which both DF and AF protocols are examined. To determine the decoding order of cell-edge users' data, they adopt statistical channel state information (CSI) for such system and the closed form of the ergodic sum rate and outage probability are derived. In a similar trend, the authors in [19] developed new closed-form expressions of both precise and approximate outage probabilities of fixed gain AF relaying in NOMA.

In this study, we consider a different model compared with [19, 30], where an FD relay supports transmission data from the base station (BS) in the scenario of NOMA to serve two NOMA users with different locations assigned, including the users at the cell center and the other one located in the cell edge. It is worth noting that our work considers the same architecture as that in [9, 17]. However, compared to work in [9] which considered the Rayleigh fading environment, our investigation generalizes in the complex case of Nakagami-m fading condition. Furthermore, research [17] is assumed under perfect co-channel suppression at user and modelled nonfading self-interference channel as a Gaussian noise for convenience in analysis. These assumptions are extended in this work by exploiting more practical scenario of imperfect channel estimation and self-interference cancellation scheme. Unlike the conventional NOMA performed in previous works [19, 30], this investigation mainly focuses on two cases of relay where single antenna or dual antenna are equipped at relay to perform forwarding NOMA signals to destination. The contributions are summarized as follows:

(i) We investigate the outage performance for NOMA systems with the proposed FD relaying strategy, and it is derived in the closed form for the considering scenario. On the contrary, the performance comparisons among proposed NOMA, with FD and half-duplex (HD) relaying schemes are also provided.

(ii) We examine the achievable throughput based on the derived outage probability. To look insights regarding energy, we consider energy efficiency performance for the proposed system model.

(iii) Computer simulations are conducted to verify the accuracy of the theoretical analyses. Main results show that NOMA with the higher fading parameter and higher transmitting power of the BS outperforms the remaining cases in terms of outage performance and throughput. Such results exhibit a better behavior in NOMA with the improved channel condition, especially in the high transmitting power region.

The remaining of this paper is organized as follows. The overall system model and assumptions are introduced in Section 2. In addition, Sections 3 and 4 represent the detail analytical derivations of the outage probability for FD and HD transmission mode, respectively. In Section 5 provides

simulation results, and Section 6 provides a conclusion for this research.

2. System and Signal Model

2.1. Network Topology and Channel Assumptions

2.1.1. Network Topology. The considered FD cooperative relaying NOMA network is depicted in Figure 1, where a base station assigned with single antenna, denoted by B, transfers the information toward two single antenna equipment users, U_1 and U_2, by exploiting the power domain division technique, namely, NOMA. In such a model, it is assumed that existence of the $B \longrightarrow U_1$ link can be seen due to nearer distance, while the connection of $B \longrightarrow U_2$ link is nonexistence. Hence, B directly transmits messages to U_1 and indirectly sends to U_2 with help of the intermediate relay node which is denoted by $\mathscr{R}$. Specially, in order to enhance the spectral efficiency, $\mathscr{R}$ is designed to operate in the full-duplex mode and thus $\mathscr{R}$ facilitates two antennas as assumed in [9, 17]. It is worth noting that the multiple antenna relay node can further mitigate the self-interference power; however, this approach leads system to be more complex [31]. Thus, we assume the single antenna for transmitting and receiving at terminals in this work. It can refer as a typical situation of a multiantenna scheme as investigated in [9, 17].

2.1.2. Outdated Channel Model. In practice, because of estimation errors, it is highly difficult to estimate the perfect channel state information (CSI) of wireless network. Thus, the outdated channel coefficient is modelled as follows [32, 33]:

$$\widehat{z} = z + \Delta_z, \tag{1}$$

where $\widehat{z}$ represents the outdated CSI at the transceiver with variance $\lambda_{\hat{z}}$, whereas z is the perfect channel coefficient, and Δ_z denotes the estimated channel error which can be approximated as a Gaussian random variable with zero mean and variance δ_z, and $\delta_z = \lambda_{\hat{z}} - \lambda_z$ [33], respectively. In fact, the known channel factor at the transmitter is a feedback from receiver after estimating the period; hence, the CSI at the transmitter is outdated.

2.1.3. Channel Statistic Distribution. In this work, all estimated channel coefficients are modelled under Nakagami-m fading condition. Although the Rician fading environment is more suitable to examine the self-interference (SI) link due to the short distance between antennas, its complicated distribution functions prevent to give the analytical expressions. Fortunately, the Nakagami-m fading distribution provides an alternate approximation to the Rician distribution. Inspired by this, and to simplify the analysis, we have adopted the Nakagami-m fading to model the SI channel as in this paper and recent works [6, 22]. Thus, the probability density function (PDF) and cumulative distribution function (CDF) of their gains follow gamma distributions with

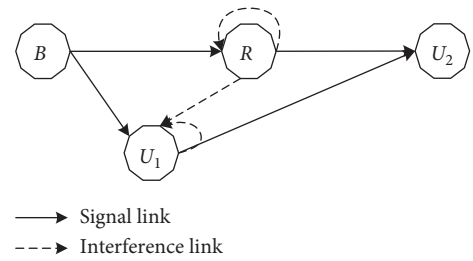

Figure 1: The full-duplex-aided relaying dual-user NOMA system model.

mean λ_z and integer severity factor m and, respectively, formulated as

$$f_z(x) = \frac{m_z^{m_z} x^{m_z - 1}}{\Gamma(m_z)\lambda_z^{m_z}} \exp\left(-\frac{m_z x}{\lambda_z}\right), \tag{2}$$

$$\begin{aligned} F_z(x) &= 1 - \frac{\Gamma(m_z, m_z x/\lambda_z)}{\Gamma(m_z)} \\ &= 1 - \exp\left(-\frac{m_z x}{\lambda_z}\right) \sum_{i=0}^{m_z - 1} \left(\frac{m_z}{\lambda_z}\right)^i \frac{x^i}{i!}, \end{aligned} \tag{3}$$

where m_z and λ_z present the fading severity factor and mean, respectively. In this paper, we also assume m_z is an integer number and $m_z \geq 1$. When $m_z = 1$, the channel environment returns to the Rayleigh fading channel. It implies that the considered Nakagami-m fading channels are more general than the previous Rayleigh fading condition. The equality in (3) is achieved by applying an equivalent relationship in Eq. 8.352.6 of [34].

Additionally, the channel coefficients are denoted as follows: the channels from B to U_1 and from B to $\mathscr{R}$ are h_1 and h_r, respectively. The connection between $\mathscr{R}$ (or U_1) and U_2 be g_2 (or g_1), while the self-interference link at $\mathscr{R}$ and interference of $\mathscr{R} \longrightarrow U_1$ link are symbolized as f_r and f_1, respectively. In general, the channel gain $|x|^2$ follows the gamma distribution with parameter m_x and λ_x with $x \in \{h_1, h_r, g_2, g_1, f_r, f_1\}$.

Remark 1. It is noted that, although the considered system in this study is as same as in [9, 17], the channel conditions investigated in our system undergo imperfect knowledge of the Nakagami-m fading environment. Since such channel condition is more general than the Rayleigh fading environment in [9], and this research can be considered as a generalized version of previous work in [17] when considering nonideal interference cancellation hardware for both co-channel interference at U_1 and self-interference at $\mathscr{R}$, taking imperfect CSI noise into account.

Remark 2. In this paper, the severity fading parameter, i.e., m, is strictly supposed as an integer value. Thus, the analytical expression is only true for such considerations. The general case of noninterger values of m is beyond the scope of this study.

2.2. Full-Duplex NOMA Relaying Scheme and Signal Analysis

2.2.1. Cooperative NOMA FD Relaying Scheme. In this part, we adopt cooperative FD relaying NOMA network considered in [9, 17]. The modelling signal can be formulated as follows. In the block time t, B sends a superimposed mixture of the signals intended for both U_1 and U_2, thanks to the power domain division:

$$s(t) = \sqrt{a_1}x_1(t) + \sqrt{a_2}x_2(t), \tag{4}$$

where a_1 and a_2 are two allocated power parameters for U_1 and U_2 messages, respectively, with $a_1 + a_2 = 1$ and, $a_1, a_2 \geq 0$. As aforementioned, we assume that U_1 is the near user and U_2 is the far user, thus it satisfies $a_1 < a_2$. The notations x_1, x_2, and s are analogously U_1 and U_2 and superimposed NOMA data symbols, with zero mean and variances of unit.

Firstly, we consider the signal associated with U_1. According to $B \longrightarrow U_1$ link, the received signal at U_1 under imperfect CSI is thus given by

$$y_{U_1}(t) = \sqrt{P_B}\left(h_1 + \Delta_{h_1}\right)s(t) + \sqrt{P_{\mathscr{R}}}\left(f_1 + \Delta_{f_1}\right)x_2(t - \widehat{t}\,) + n_{U_1}(t), \tag{5}$$

where P_B and $P_{\mathscr{R}}$ are B and $\mathscr{R}$ transmission powers, respectively. n_{U_1} denotes the additive white Gaussian noise (AWGN) at U_1 with zero mean and variance N_0. Besides, f_1 denotes the residual interference coefficient after using interference cancellation technique in the FD mode. It is worth pointing out that user U_1 must first detect message x_2 for SIC purpose so, therefore, user U_1 can theoretically remove interference signal x_2 which was sent from the relay node. However, the interference part cannot completely suppress due to the limitation of mitigation level and imperfect CSI. Then, they are treated as residual interference signals at U_1 as that in [9]. We use $\widehat{t}$ to represent the delay time for signal processing. Its value is small compared to time block and can be ignored in analysis as that in [9].

Based on NOMA principle, the near user U_1 first detects the U_2 message by treating U_1 symbol as interference, then removes U_2 symbol, and finally decodes its own data. Therefore, the signal to interference plus noise ratio (SINR) to decode U_2 message at U_1 is

$$\gamma_{U_2,U_1} = \frac{a_2\rho_B|h_1|^2}{\rho_B a_1|h_1|^2 + \rho_{\mathscr{R}}|f_1|^2 + \sigma_{U_1}}, \tag{6}$$

and the SINR at U_1 to detect its own data is given by

$$\gamma_{U_1,U_1} = \frac{a_1\rho_B|h_1|^2}{\rho_{\mathscr{R}}|f_1|^2 + \sigma_{U_1}}, \tag{7}$$

where $\rho_B = P_B/N_0$ and $\rho_{\mathscr{R}} = P_{\mathscr{R}}/N_0$ are the signal-to-noise ratio (SNR) at B and $\mathscr{R}$, respectively, and $\sigma_{U_1} \triangleq \rho_B\delta_{h_1} + \rho_{\mathscr{R}}\delta_{f_1} + 1$. It is worth noting that, in (7), we assume the perfect SIC is achieved as that in [9]. The system performance can be degraded since successive interference was cancelled imperfectly. But it is out of the paper scope.

Now, considering the $B \longrightarrow \mathscr{R} \longrightarrow U_2$ connection, by denoting channel coefficients of $B \longrightarrow \mathscr{R}$, $\mathscr{R} \longrightarrow U_2$, and relay loop interference links as h_2, g_2, and f_r, respectively, the received signal at $\mathscr{R}$ is expressed as

$$y_{\mathscr{R}}(t) = \sqrt{P_B}\left(h_2 + \Delta_{h_2}\right)s(t) + \sqrt{P_{\mathscr{R}}}\left(f_r + \Delta_{f_r}\right)x_2(t - \widehat{t}\,) + n_{\mathscr{R}}(t), \tag{8}$$

and the amount of signals received at U_2 from relay node could be formulated as

$$y_{U_2}(t) = \sqrt{P_{\mathscr{R}}}\left(g_2 + \Delta_{g_2}\right)x_2(t - \widehat{t}\,) + n_{U_2}(t), \tag{9}$$

where $n_{\mathscr{R}}$ and n_{U_2} are AWGNs at relay and U_2, respectively, both with zero mean and variance N_0. Since the relay tries to decode the information intended for U_2 while treating the symbol of U_1 as interference, the SINR is computed to decode the message of U_2, and it can be expressed as

$$\gamma_{U_2,\mathscr{R}} = \frac{a_2\rho_B|h_2|^2}{a_1\rho_B|h_2|^2 + \rho_{\mathscr{R}}|f_r|^2 + \sigma_{\mathscr{R}}}. \tag{10}$$

Additionally, from (9), the SNR to detect message at U_2 is

$$\gamma_{U_2,U_2} = \frac{\rho_{\mathscr{R}}|g_2|^2}{\sigma_{U_2}}, \tag{11}$$

where $\sigma_{\mathscr{R}} \triangleq \rho_B\delta_{h_2} + \rho_{\mathscr{R}}\delta_{f_r} + 1$ and $\sigma_{U_2} \triangleq \rho_{\mathscr{R}}\delta_{g_2} + 1$.

2.2.2. The Near NOMA User-Aided Cooperative NOMA FD Relaying Scheme. In this subsection, we combine the user-aided relaying architecture in [10] into FD cooperative. This idea exploits the near user U_1 as a relay node to forward message to far user U_2. In fact, U_1 first decodes x_2 symbol for SIC purpose; hence, U_1 can forward it to improve U_2 decode diversity. In such a suggested scheme, SINRs at U_1 for detecting the U_2 data become

$$\gamma^{\text{pro}}_{U_2,U_1} = \frac{a_2\rho^{\text{pro}}_B|h_1|^2}{\rho^{\text{pro}}_B a_1|h_1|^2 + \rho^{\text{pro}}_{\mathscr{R}}|f_1|^2 + \rho^{\text{pro}}_{U_1}|f_{U_1}|^2 + \sigma^{\text{pro}}_{U_1}}, \tag{12}$$

where $\rho^{\text{pro}}_X \triangleq P^{\text{pro}}_X/N_0$, $X \in \{B, \mathscr{R}, U_1\}$ with P_X the transmitting power at node X and $\sigma^{\text{pro}}_{U_1} \triangleq \sigma_{U_1} + \rho^{\text{pro}}_{U_1}\delta_{f_{U_1}}$. In addition, the SINR to detect data x_1 at U_1 is reexpressed as

$$\gamma^{\text{pro}}_{U_1,U_1} = \frac{a_1\rho^{\text{pro}}_B|h_1|^2}{\rho^{\text{pro}}_{\mathscr{R}}|f_1|^2 + \rho^{\text{pro}}_{U_1}|f_{U_1}|^2 + \sigma^{\text{pro}}_{U_1}}. \tag{13}$$

According to user-aided transmission, the SINR at relay to determine x_2 is now suffered by additive interference intended from U_1 caused by FD forwarding and can be rewritten by

$$\gamma^{\text{pro}}_{U_2,\mathscr{R}} = \frac{a_2\rho^{\text{pro}}_B|h_2|^2}{a_1\rho^{\text{pro}}_B|h_2|^2 + \rho^{\text{pro}}_{\mathscr{R}}|f_r|^2 + \rho^{\text{pro}}_{U_1}|f_2|^2 + \sigma^{\text{pro}}_{\mathscr{R}}}, \tag{14}$$

where $\sigma^{\text{pro}}_{\mathscr{R}} \triangleq \rho^{\text{pro}}_{U_1}\delta_{f_2} + \sigma_{\mathscr{R}}$.

Regarding the $B \longrightarrow \mathscr{R} \longrightarrow U_2$ link, the SINR at relay and U_2 are given by adding the interference from aided user U_1 as

$$\gamma_{U_2,\mathscr{R}}^{\text{pro}} = \frac{a_2\rho_B^{\text{pro}}|h_2|^2}{a_1\rho_B^{\text{pro}}|h_2|^2 + \rho_{\mathscr{R}}^{\text{pro}}|f_r|^2 + \rho_{U_1}^{\text{pro}}|f_2|^2 + \sigma_{\mathscr{R}}^{\text{pro}}},$$
$$\gamma_{U_2,U_2}^{\mathscr{R},\text{pro}} = \frac{\rho_{\mathscr{R}}^{\text{pro}}|g_2|^2}{\sigma_{U_2}^{\text{pro}}}, \tag{15}$$

where $\sigma_{\mathscr{R}}^{\text{pro}} \triangleq \rho_{U_1}\delta_{f_2} + \sigma_{\mathscr{R}}$ and $\sigma_{U_2}^{\text{pro}} \triangleq \rho_{\mathscr{R}}^{\text{pro}}\delta_{g_2} + 1$.

Moreover, the listened signal at U_2 from U_1 could be expressed as

$$y_{U_2}^{U_1,\text{pro}}(t) = \sqrt{P_{U_1}^{\text{pro}}}\left(g_1 + \Delta_{g_1}\right)x_2(t-\widehat{t}) + n_{U_2}(t). \tag{16}$$

Then, the SNR at U_2 from user-aided relaying U_1 is

$$\gamma_{U_2,U_2}^{U_1,\text{pro}} = \frac{\rho_{U_1}^{\text{pro}}|g_1|^2}{\sigma_{U_2}^{U_1,\text{pro}}}, \tag{17}$$

with $\sigma_{U_2}^{U_1,\text{pro}} \triangleq \rho_{U_1}^{\text{pro}}\delta_{g_1} + 1$. For simplicity in analysis, it is assumed that the far user U_2 exploits the selection combine (SC) approach to process two paths achieved from the relay and user-aided relaying U_1. Hence, the SINR at U_2 with the proposed scheme is expressed as

$$\gamma_{U_2,U_2}^{\text{pro}} = \max\left(\gamma_{B,\mathscr{R},U_2}^{\text{pro}}, \gamma_{B,U_1,U_2}^{\text{pro}}\right), \tag{18}$$

where $\gamma_{B,\mathscr{R},U_2}^{\text{pro}} \triangleq \min(\gamma_{U_2,\mathscr{R}}^{\text{pro}}, \gamma_{U_2,U_2}^{\mathscr{R},\text{pro}})$ and $\gamma_{B,U_1,U_2}^{\text{pro}} \triangleq \min(\gamma_{U_2,U_1}^{\text{pro}}, \gamma_{U_2,U_2}^{U_1,\text{pro}})$.

In the sequels, the system performance in terms of outage probability will be analysed.

3. Outage Probability Consideration on Full-Duplex Relaying NOMA

3.1. Outage Probability of U_1

3.1.1. Cooperative NOMA FD Relaying Scheme. According to the considered NOMA technique, the outage probability of U_1 can be determined as error when recognizing either U_2 or its own message. Thus, the U_1 meets outage probability, $\mathscr{OP}_{U_1}$, which is formulated as

$$\begin{aligned}\mathscr{OP}_{U_1} &= \Pr\left\{C_{U_2,U_1} < R_2 \text{ or}, C_{U_1,U_1} < R_1\right\} \\ &= 1 - \Pr\left\{C_{U_2,U_1} \geq R_2 \text{ and }, C_{U_1,U_1} \geq R_1\right\},\end{aligned} \tag{19}$$

where R_1 and R_2 are the target rates of U_2 and U_1, respectively, and $C_{U_2,U_1} \triangleq \log_2(1+\gamma_{U_2,U_1})$ and $C_{U_1,U_1} \triangleq \log_2(1+\gamma_{U_1,U_1})$ are the channel capacities at U_1 associated with U_2 and U_1 symbols, respectively.

Proposition 1. *Putting $\gamma_{\text{th},U_1} = 2^{R_1} - 1$ and $\gamma_{\text{th},U_2} = 2^{R_2} - 1$. ie outage probability of U_1 for such a considered system over the Nakagami-m fading condition is given by*

$$\mathscr{OP}_{U_1} = \begin{cases} 1, & \vartheta \leq 0, \\ 1 - \psi\sum_{i=0}^{m_{h_1}-1}\sum_{k=0}^{i}\binom{i}{k}\dfrac{\omega^i\sigma_{U_1}^{i-k}\rho_{\mathscr{R}}^k\Gamma\left(k+m_{f_1}\right)}{i!\Omega_{f_1}^{k+m_{f_1}}}, & \vartheta > 0, \end{cases} \tag{20}$$

where $\vartheta = \min(a_2/\gamma_{\text{th},U_2} - a_1, a_1/\gamma_{\text{th},U_1})$, $\omega = m_{h_1}/(\rho_B\vartheta\lambda_{h_1})$, $\Omega_{f_1} = \rho_{\mathscr{R}}\omega + m_{f_1}/\lambda_{f_1}$, *and* $\psi = e^{-\sigma_{U_1}\omega}m_{f_1}^{m_{f_1}}/(\Gamma(m_{f_1})\lambda_{f_1}^{m_{f_1}})$, $\binom{i}{k} = i!/k!(i-k)!$.

Proof 1. See Appendix.

With the high SNR regime, i.e., $\sigma_{U_1}/\rho_B \longrightarrow 0$, and the approximate expression $e^x \approx 1 + x$ for $x \longrightarrow 0$, we can achieve the approximation as

$$\begin{aligned}\mathscr{OP}_{U_1} &\approx 1 - \frac{m_{f_1}^{m_{f_1}}\left(1-\sigma_{U_1}\omega\right)}{\Gamma\left(m_{f_1}\right)\lambda_{f_1}^{m_{f_1}}}\sum_{i=0}^{m_{h_1}-1}\omega^i\int_0^\infty x^{m_{f_1}-1}e^{-\Omega_{f_1}x} \\ &\quad\cdot\frac{(\rho_{\mathscr{R}}x)^i}{i!}dx \\ &= 1 - \frac{m_{f_1}^{m_{f_1}}\left(1-\sigma_{U_1}\omega\right)}{\Gamma\left(m_{f_1}\right)\lambda_{f_1}^{m_{f_1}}}\sum_{i=0}^{m_{h_1}-1}\frac{\omega^i\rho_R^i\Gamma\left(i+m_{f_1}\right)}{i!\Omega_{f_1}^{i+m_{f_1}}}.\end{aligned} \tag{21}$$

Starting from (A.2), we can achieve the asymptotic expression as

$$\begin{aligned}\mathscr{OP}_{U_1}^{\infty} &\longrightarrow 1 - \int_0^\infty\left(1 - F_{|h_1|^2}\left(\frac{\rho_{\mathscr{R}}x}{\rho_B\vartheta}\right)\right)f_{|f_1|^2}(x)\,dx \\ &= 1 - \frac{m_{f_1}^{m_{f_1}}}{\Gamma\left(m_{f_1}\right)\lambda_{f_1}^{m_{f_1}}}\frac{1}{\Gamma\left(m_{h_1}\right)}\int_0^\infty\Gamma\left(m_{h_1},\rho_R\omega x\right)x^{m_{f_1}-1} \\ &\quad\cdot\exp\left(-\frac{m_{f_1}x}{\lambda_{f_1}}\right)dx.\end{aligned} \tag{22}$$

Finally, by applying Eq. 6.455.1 of [34] for the last integral, the asymptotic outage probability of U_1 is given by

$$\begin{aligned}\mathscr{OP}_{U_1}^{\infty} &\longrightarrow 1 - \frac{m_{f_1}^{m_{f_1}-1}\Gamma\left(m_{f_1}+m_{h_1}\right)}{\Gamma\left(m_{f_1}\right)\Gamma\left(m_{h_1}\right)\lambda_{f_1}^{m_{f_1}}}(\omega\rho_R)^{m_{h_1}}\Omega_{f_1}^{-m_{f_1}-m_{h_1}} \\ &\quad\times{}_2F_1\left(1, m_{f_1}+m_{h_1}; m_{f_1}+1; \frac{m_{f_1}}{\lambda_{f_1}\Omega_{f_1}}\right),\end{aligned} \tag{23}$$

where ${}_2F_1(a,b;c;d)$ is the Gaussian hypergeometric function [34].

3.1.2. User-Aided Cooperative NOMA FD Relaying Scheme. Similar to that in (19), the outage probability of U_1 can be obtained by replacing the corresponding proposed scheme SINR instead and is given by

$$\mathcal{OP}_{U_1}^{\text{pro}} = 1 - \Pr\left\{\gamma_{U_1,U_1}^{\text{pro}} \geq \gamma_{\text{th},U_1} \text{ and }, \gamma_{U_2,U_1}^{\text{pro}} \geq \gamma_{\text{th},U_2}\right\}. \quad (24)$$

Substituting (12) and (13) into (24), the U_1 outage performance is given in Proposition 2.

Proposition 2. *The outage probability of U_1 for the user-aided relaying cooperative FD relay system under the Nakagami-m fading environment is determined as*

$$\mathcal{OP}_{\mathcal{U}_1}^{\text{pro}} = \begin{cases} 1, & \vartheta \leq 0, \\ 1 - \psi_{U_1}^{\text{pro}} \sum_{i=0}^{m_{h_1}-1} \sum_{k=0}^{i} \sum_{n=0}^{k} \binom{i}{k}\binom{k}{n} \Xi_{i,k,n}, & \vartheta > 0, \end{cases} \quad (25)$$

where ϑ is defined in Proposition 1, $\omega^{\text{pro}} = m_{h_1}/(\rho_B^{\text{pro}}\vartheta\lambda_{h_1})$, $\Omega_{f_1}^{\text{pro}} = \rho_{\mathcal{R}}^{\text{pro}}\omega^{\text{pro}} + m_{f_1}/\lambda_{f_1}$, and $\Omega_{f_{U_1}}^{\text{pro}} \triangleq m_{f_{U_1}}/\lambda_{f_{U_1}} + \rho_{U_1}^{\text{pro}}\omega^{\text{pro}}$:

$$\psi_1^{\text{pro}} \triangleq \frac{e^{-\omega^{\text{pro}}\sigma_{U_1}^{\text{pro}}} m_{f_{U_1}}^{m_{f_{U_1}}} m_{f_1}^{m_{f_1}}}{\Gamma\left(m_{f_{U_1}}\right)\Gamma\left(m_{f_1}\right)\lambda_{f_{U_1}}^{m_{f_{U_1}}}\lambda_{f_1}^{m_{f_1}}},$$

$$\Xi_{i,k,n} \triangleq \frac{(\omega^{\text{pro}})^i\left(\sigma_{U_1}^{\text{pro}}\right)^{i-k}\left(\rho_{\mathcal{R}}^{\text{pro}}\right)^n\left(\rho_{U_1}^{\text{pro}}\right)^{k-n}}{i!\left(\Omega_{f_1}^{\text{pro}}\right)^{n+m_{f_1}}\left(\Omega_{f_{U_1}}^{\text{pro}}\right)^{k+m_{f_{U_1}}-n}} \times \Gamma\left(n+m_{f_1}\right)\Gamma\left(k+m_{f_{U_1}}-n\right). \quad (26)$$

Proof 2. The procedure is similar that in Appendix.

In case of $\vartheta > 0$, we get the approximate expression:

$$\mathcal{OP}_{U_1}^{\text{pro}} \approx 1 - \frac{m_{f_{U_1}}^{m_{f_{U_1}}} m_{f_1}^{m_{f_1}}\left(1-\omega^{\text{pro}}\sigma_{U_1}^{\text{pro}}\right)}{\Gamma\left(m_{f_{U_1}}\right)\Gamma\left(m_{f_1}\right)\lambda_{f_{U_1}}^{m_{f_{U_1}}}\lambda_{f_1}^{m_{f_1}}} \sum_{i=0}^{m_{h_1}-1}\sum_{k=0}^{i}\binom{i}{k}\Xi_{i,k}, \quad (27)$$

where

$$\Xi_{i,k} = \frac{(\omega^{\text{pro}})^i\left(\rho_R^{\text{pro}}\right)^k\left(\rho_{U_1}^{\text{pro}}\right)^{i-k}}{i!\left(\Omega_{f_1}^{\text{pro}}\right)^{k+m_{f_1}}\left(\Omega_{f_{U_1}}^{\text{pro}}\right)^{i+m_{f_{U_1}}-k}} \cdot \Gamma\left(k+m_{f_1}\right)\Gamma\left(i+m_{f_{U_1}}-k\right). \quad (28)$$

3.2. Outage Probability of U_2

3.2.1. Cooperative NOMA FD Relaying Scheme. Based on the operation of the dual-hop cooperative DF relaying scheme, the outage probability of U_2 can be expressed as

$$\mathcal{OP}_{U_2} = \Pr\left\{\min\left(C_{U_2,\mathcal{R}}, C_{U_2,U_2}\right) < R_2\right\} = 1 - \Pr\left\{\min\left(\gamma_{U_2,\mathcal{R}}, \gamma_{U_2,U_2}\right) \geq \gamma_{\text{th},U_2}\right\}, \quad (29)$$

where $C_{U_2,\mathcal{R}} \triangleq \log_2(1+\gamma_{U_2,\mathcal{R}})$ and $C_{U_2,U_2} \triangleq \log_2(1+\gamma_{U_2,U_2})$ are the channel capacities of U_2 message associated with $B \longrightarrow \mathcal{R}$ hop and $\mathcal{R} \longrightarrow U_2$ hop, respectively. It is worth noting that γ_{th,U_2} is defined in Proposition 1.

Proposition 3. *We denote $\vartheta_2 = a_2/\gamma_{\text{th},U_2} - a_1$, $\omega_2 = m_{h_2}/\rho_B\vartheta_2\lambda_{h_2}$, $\Omega_2 = \rho_{\mathcal{R}}\omega_2 + m_{f_r}/\lambda_{f_r}$, and $\psi_2 = e^{-\sigma_{\mathcal{R}}\omega_2} m_{f_r}^{m_{f_r}}/(\Gamma(m_{f_r})\lambda_{f_r}^{m_{f_r}})$, and the outage probability of U_2 is given by*

$$\mathcal{OP}_{U_2} = \begin{cases} 1, & \vartheta_2 \leq 0, \\ 1 - \Upsilon_{U_2,1} \times \Upsilon_{U_2,2}, & \vartheta_2 > 0, \end{cases} \quad (30)$$

where $\Upsilon_{U_2,2} = 1/\Gamma(m_{g_2})\Gamma(m_{g_2}, m_{g_2}\sigma_{U_2}\gamma_{th,U_2}/\rho_{\mathcal{R}}\lambda_{g_2})$ and

$$\Upsilon_{U_2,1} = \psi_2 \sum_{i=0}^{m_{h_2}-1}\sum_{k=0}^{i}\binom{i}{k}\frac{\omega_2^i\sigma_{\mathcal{R}}^{i-k}\rho_{\mathcal{R}}^k\Gamma\left(k+m_{f_r}\right)}{i!\Omega_2^{k+m_{f_r}}}. \quad (31)$$

Proof 3. See in Appendix.

The approximate expression is given as

$$\Upsilon_{U_2,1} \approx 1 - \frac{(1-\sigma_{\mathcal{R}}\omega_2)m_{f_r}^{m_{f_r}}}{\Gamma\left(m_{f_r}\right)\lambda_{f_r}^{m_{f_r}}} \sum_{i=0}^{m_{h_2}-1}\frac{\omega_2^i\rho_R^i\Gamma\left(i+m_{f_r}\right)}{i!\Omega_2^{i+m_{f_r}}},$$

$$\Upsilon_{U_2,1}^{\infty} \longrightarrow 1 - \frac{m_{f_r}^{m_{f_r}-1}\Gamma\left(m_{f_r}+m_{h_2}\right)}{\Gamma\left(m_{f_r}\right)\Gamma\left(m_{h_2}\right)\lambda_{f_r}^{m_{f_r}}}\frac{(\omega_2\rho_R)^{m_{h_2}}}{\Omega_2^{m_{f_r}+m_{h_2}}} \times {}_2F_1\left(1, m_{f_r}+m_{h_2}; m_{f_r}+1; \frac{m_{f_r}}{\lambda_{f_r}\Omega_2}\right). \quad (32)$$

With the help of equality in Eq. 8.354.2 of [34], since $\rho_{\mathcal{R}} \longrightarrow \infty$, we can get

$$\Upsilon_{U_2,2} \approx 1 - \frac{m_{g_2}^{m_{g_2}-1}}{\Gamma\left(m_{g_2}\right)}\left(\frac{\sigma_{U_2}\gamma_{\text{th},U_2}}{\rho_{\mathcal{R}}\lambda_{g_2}}\right)^{m_{g_2}}. \quad (33)$$

3.2.2. User-Aided Cooperative NOMA FD Relaying Scheme. As early assumption, U_2 shall exploit the SC technique to choose the best from both signal paths. Additionally, channels are independent with each other, and the outage can be further written as

$$\mathcal{OP}_{U_2}^{\text{pro}} = \Pr\left\{\gamma_{U_2,U_2}^{\text{pro}} < \gamma_{\text{th},U_2}\right\} = \left(1 - \Pr\left(\gamma_{U_2,\mathcal{R}}^{\text{pro}} \geq \gamma_{\text{th},U_2}\right)\Pr\left(\gamma_{U_2,U_2}^{\text{pro}} \geq \gamma_{\text{th},U_2}\right)\right) \times \left(1 - \Pr\left(\gamma_{U_2,U_1}^{\text{pro}} \geq \gamma_{\text{th},U_2}\right)\Pr\left(\gamma_{U_2,U_2}^{U_1,\text{pro}} \geq \gamma_{\text{th},U_2}\right)\right). \quad (34)$$

Proposition 4. *The outage probability of U_2 for the suggested U_1-aided FD relaying cooperative NOMA system is given by*

$$\mathcal{OP}_{U_2}^{\text{pro}} = \begin{cases} 1, & \vartheta_2 \le 0, \\ \left(1 - \Upsilon_{U_2,1}^{U_1,\text{pro}} \times \Upsilon_{U_2,2}^{U_1,\text{pro}}\right)\left(1 - \Upsilon_{U_2,1}^{\mathcal{R},\text{pro}} \times \Upsilon_{U_2,2}^{\mathcal{R},\text{pro}}\right), & \vartheta_2 > 0, \end{cases} \tag{35}$$

where

$$\begin{aligned}
\Upsilon_{U_2,2}^{\mathcal{R},\text{pro}} &\triangleq \frac{1}{\Gamma(m_{g_2})}\Gamma\left(m_{g_2}, \frac{m_{g_2}\sigma_{U_2}^{\text{pro}}\gamma_{\text{th},U_2}}{\rho_{\mathcal{R}}^{\text{pro}}\lambda_{g_2}}\right) \\
&\approx 1 - \frac{m_{g_2}^{m_{g_2}-1}}{\Gamma(m_{g_2})}\left(\frac{\sigma_{U_2}^{\text{pro}}\gamma_{\text{th},U_2}}{\rho_{\mathcal{R}}^{\text{pro}}\lambda_{g_2}}\right)^{m_{g_2}}, \\
\Upsilon_{U_2,1}^{\mathcal{R},\text{pro}} &\triangleq \psi_{\mathcal{R}}^{\text{pro}} \sum_{i=0}^{m_{h_2}-1}\sum_{k=0}^{i}\sum_{n=0}^{k}\binom{i}{k}\binom{k}{n}\Gamma\left(k + m_{f_r} - n\right) \\
&\quad \times \Gamma\left(n + m_{f_2}\right)\frac{\left(\omega_{2,g_2}^{\text{pro}}\right)^i\left(\sigma_{\mathcal{R}}^{\text{pro}}\right)^{i-k}\left(\rho_{\mathcal{R}}^{\text{pro}}\right)^n\left(\rho_{U_1}^{\text{pro}}\right)^{k-n}}{i!\left(\Omega_{f_r}^{\text{pro}}\right)^{n+m_{f_2}}\left(\Omega_{f_2}^{\text{pro}}\right)^{k+m_{f_r}-n}}, \\
\Upsilon_{U_2,2}^{U_1,\text{pro}} &\triangleq \frac{1}{\Gamma(m_{g_1})}\Gamma\left(m_{g_1}, \frac{m_{g_1}\sigma_{U_2}^{U_1,\text{pro}}\gamma_{\text{th},U_2}}{\rho_{U_1}^{\text{pro}}\lambda_{g_1}}\right) \\
&\approx 1 - \frac{m_{g_1}^{m_{g_1}-1}}{\Gamma(m_{g_1})}\left(\frac{\sigma_{U_2}^{U_1,\text{pro}}\gamma_{\text{th},U_2}}{\rho_{\mathcal{R}}^{\text{pro}}\lambda_{g_1}}\right)^{m_{g_1}}, \\
\Upsilon_{U_2,1}^{U_1,\text{pro}} &\triangleq \psi_{U_1}^{\text{pro}} \sum_{i=0}^{m_{h_1}-1}\sum_{k=0}^{i}\sum_{n=0}^{k}\binom{i}{k}\binom{k}{n}\Gamma\left(k + m_{f_{U_1}} - n\right) \\
&\quad \times \Gamma\left(n + m_{f_1}\right)\frac{\left(\omega_{2,g_1}^{\text{pro}}\right)^i\left(\sigma_{U_1}^{\text{pro}}\right)^{i-k}\left(\rho_{\mathcal{R}}^{\text{pro}}\right)^n\left(\rho_{U_1}^{\text{pro}}\right)^{k-n}}{i!\left(\Omega_{f_1}^{\text{pro}}\right)^{n+m_{f_1}}\left(\Omega_{f_{U_1}}^{\text{pro}}\right)^{k+m_{f_{U_1}}-n}},
\end{aligned} \tag{36}$$

with ϑ_2 *defined in Proposition 3,* $\omega_{2,g_1}^{\text{pro}} = m_{g_1}/(\rho_B^{\text{pro}}\vartheta_2\lambda_{g_1})$, $\omega_{2,g_2}^{\text{pro}} = m_{g_2}/\rho_B^{\text{pro}}\vartheta_2\lambda_{g_2}$, $\Omega_{2,f_1}^{\text{pro}} = \rho_{\mathcal{R}}^{\text{pro}}\omega_2^{\text{pro}} + m_{f_1}/\lambda_{f_1}$, $\Omega_{2,f_2}^{\text{pro}} = \rho_{U_1}^{\text{pro}}\omega_2^{\text{pro}} + m_{f_2}/\lambda_{f_2}$, $\Omega_{2,f_r}^{\text{pro}} = \rho_{\mathcal{R}}^{\text{pro}}\omega_2^{\text{pro}} + m_{f_r}/\lambda_{f_r}$, $\Omega_{2,f_{U_1}}^{\text{pro}} = \rho_{U_1}^{\text{pro}}\omega_2^{\text{pro}} + m_{f_{U_1}}/\lambda_{f_{U_1}}$, $\psi_{\mathcal{R}}^{\text{pro}} \triangleq e^{-\omega_{2,h_2}^{\text{pro}}\sigma_{\mathcal{R}}^{\text{pro}}} m_{f_r}^{m_{f_r}} m_{f_2}^{m_{f_2}}/\Gamma(m_{f_r})\Gamma(m_{f_2})\lambda_{f_r}^{m_{f_r}}\lambda_{f_2}^{m_{f_2}}$, *and* $\psi_{U_1}^{\text{pro}} \triangleq e^{-\omega_{2,h_1}^{\text{pro}}\sigma_{U_1}^{\text{pro}}} m_{f_{U_1}}^{m_{f_{U_1}}} m_{f_1}^{m_{f_1}}/\Gamma(m_{f_{U_1}})\Gamma(m_{f_1})\lambda_{f_{U_1}}^{m_{f_{U_1}}}\lambda_{f_1}^{m_{f_1}}$.

Proof 4. The results can be obtained by similar way in proof 3.

Similar approximating procedure for U_1, the approximate expression for U_2 with user-aided relaying is derived.

3.3. Delay-Limited Throughput and Energy Efficiency for FD Relaying NOMA. In the delay-limit transmission mode, the system throughput is given as a function of outage probability [7, 10]. The throughput of the considered FD cooperative relaying NOMA is given by

$$\mathcal{T}_{\text{FD}}^{\text{con}} = R_1\left(1 - \mathcal{OP}_{U_1}\right) + R_2\left(1 - \mathcal{OP}_{U_2}\right). \tag{37}$$

Besides, for user-aided relaying, cooperative FD NOMA is obtained as

$$\mathcal{T}_{\text{FD}}^{\text{pro}} = R_1\left(1 - \mathcal{OP}_{U_1}^{\text{pro}}\right) + R_2\left(1 - \mathcal{OP}_{U_2}^{\text{pro}}\right). \tag{38}$$

Recently, to adapt deployment for green communications, the energy efficiency becomes a crucial factor to evaluate system efficiency. Normally, the energy efficiency of the considered system is defined as a ratio of throughput to total consumed power. For the aforementioned FD relaying NOMA system, the system energy efficiency can be illustrated as that in [10]:

$$\text{EE}_{\text{FD}}^{\text{con}} = \frac{\mathcal{T}_{\text{FD}}^{\text{con}}}{P_B + P_{\mathcal{R}}}. \tag{39}$$

Similarly, the EE of the user-aided relaying scheme is given by

$$\text{EE}_{\text{FD}}^{\text{pro}} = \frac{\mathcal{T}_{\text{FD}}^{\text{pro}}}{P_B^{\text{pro}} + P_{\mathcal{R}}^{\text{pro}} + P_{U_1}^{\text{pro}}}. \tag{40}$$

4. A Comparison Study on Half-Duplex Relaying NOMA

For the comparison purpose, the HD NOMA relaying is represented as a benchmark. Some results for the HD cooperative NOMA system can be addressed in [16]. Unlike the FD NOMA relaying architecture, the HD ones divide a data transmission period into two slots. In the first phase, the source B transmits message to U_1 and $\mathcal{R}$ based on the superposed signal in (4); thus the SINR at U_1 for retrieving U_2 data and its own data are, respectively, given by $\gamma_{U_2,U_1}^{\text{hd},t1} = a_2\rho_B|h_1|^2/a_1\rho_B|h_1|^2 + \sigma_{U_1}^{\text{hd}}$ and $\gamma_{U_1,U_1}^{\text{hd},t1} = a_1\rho_B|h_1|^2/\sigma_{U_1}^{\text{hd}}$ while the SINR at $\mathcal{R}$ to detect U_2 symbol can be expressed as $\gamma_{U_2,\mathcal{R}}^{\text{hd},t1} = a_2\rho_B|h_2|^2/a_1\rho_B|h_2|^2 + \sigma_{\mathcal{R}}^{\text{hd}}$ with $\sigma_{U_1}^{\text{hd}} \triangleq \rho_B\delta_{h_1} + 1$ and $\sigma_{\mathcal{R}}^{\text{hd}} \triangleq \rho_B\delta_{h_2} + 1$.

In the second phase, we consider two scenarios of implementation as in the FD transmission mode, such as conventional and proposed user-aided relaying for the HD cooperative NOMA system. Firstly, for the conventional cooperative NOMA network, the relay $\mathcal{R}$ regenerates and forwards signal to U_2 while the source and U_1 remain silent. Thus, the SNR at user U_2 from $\mathcal{R}$ in the latter time slot is given by $\gamma_{U_2,U_2}^{\text{hd},t2} = \rho_{\mathcal{R}}|g_2|^2/\sigma_{U_2}^{\text{hd}}$. Secondly, in the case of user U_1-aided relaying scheme, the SINR at U_2 from U_1 is $\gamma_{U_2,U_2}^{\text{hd},U_1} = \rho_{U_1}|g_1|^2/\sigma_{U_2}^{U_1,\text{hd}}$ with $\sigma_{U_2}^{\text{hd}} \triangleq \rho_{\mathcal{R}}\delta_{g_2} + 1$ and $\sigma_{U_2}^{U_1,\text{hd}} \triangleq \rho_{U_1}\delta_{g_1} + 1$. Similarly, by exploiting selection combining technique at the far user, the received SINR is given by $\gamma_{U_2,U_2}^{\text{hd,pro}} = \max(\gamma_{U_2,U_2}^{\text{hd}}, \gamma_{U_2,U_2}^{\text{hd},U_1})$. It is noted that the SINR of U_1 and U_2 for the proposed user-aided relaying HD scheme is

similar to that for the conventional HD cooperative scheme except that transmitting power is replaced by the corresponding proposed power, i.e., ρ_B^{pro}, $\rho_{\mathscr{R}}^{\text{pro}}$, and $\rho_{U_1}^{\text{pro}}$. In what follows, we will study the outage probability of considered HD networks.

4.1. Outage Probability of U_1. Regarding U_1 performance, the outage probability for the conventional scheme can be obtained as the expression below. Define $\gamma_{\text{th},U_2}^{\text{hd}} = 2^{2R_2} - 1$ and $\gamma_{\text{th},U_1}^{\text{hd}} = 2^{2R_1} - 1$. In the HD transmission mode, the outage probability of user 1 for the traditional cooperative NOMA is given by

$$\mathscr{OP}_{U_1}^{\text{hd},t1} = \begin{cases} 1, & \vartheta_{\text{hd}} \le 0, \\ 1 - \dfrac{\Gamma\left(m_{h_1}, \omega_{\text{hd}}\sigma_{U_1}^{\text{hd}}\right)}{\Gamma\left(m_{h_1}\right)}, & \vartheta_{\text{hd}} > 0, \end{cases} \tag{41}$$

where $\vartheta_{\text{hd}} = \min\left(a_2/\gamma_{\text{th},U_2}^{\text{hd}} - a_1, a_1/\gamma_{\text{th},U_1}^{\text{hd}}\right)$ and $\omega_{\text{hd}} = m_{h_1}/(\rho_B\vartheta_{\text{hd}}\lambda_{h_1})$.

For the proposed FD user U_1-aided relaying cooperative NOMA system, the outage probability is easily obtained by replacing ρ_B with ρ_B^{pro}.

4.2. Outage Probability of U_2. The outage probability of U_2 in HD conventional relaying network is obtained as

$$\mathscr{OP}_{U_2}^{\text{hd}} = \begin{cases} 1, & \vartheta_2 \le 0, \\ 1 - \dfrac{\Gamma\left(m_{h_2}, \omega_2\sigma_{\mathscr{R}}^{\text{hd}}\right)}{\Gamma\left(m_{g_2}\right)\Gamma\left(m_{h_2}\right)}\Gamma\left(m_{g_2}, \dfrac{m_{g_2}\gamma_{\text{th},U_2}^{\text{hd}}\sigma_{U_2}^{\text{hd}}}{\rho_{\mathscr{R}}\lambda_{g_2}}\right), & \vartheta_2 > 0, \end{cases} \tag{42}$$

and the outage for the proposed U_1-aided relaying cooperative HD scheme is

$$\mathscr{OP}_{U_2}^{\text{hd,pro}} = \begin{cases} 1, & \vartheta_2 \le 0, \\ \left(1 - \Upsilon_{U_2}^{\mathscr{R},\text{hd,pro}}\right) \times \left(1 - \Upsilon_{U_2}^{U_1,\text{hd,pro}}\right), & \vartheta_2 > 0, \end{cases} \tag{43}$$

where ϑ_2 and ω_2 are given in Proposition 3 and

$$\Upsilon_{U_2}^{\mathscr{R},\text{hd,pro}} \triangleq \frac{\Gamma\left(m_{h_2}, \omega_2\gamma_{\text{th},U_2}^{\text{hd}}\sigma_{\mathscr{R}}^{\text{hd}}\right)}{\Gamma\left(m_{g_2}\right)\Gamma\left(m_{h_2}\right)}\Gamma\left(m_{g_2}, \frac{m_{g_2}\gamma_{\text{th},U_2}^{\text{hd}}\sigma_{U_2}^{\text{hd}}}{\rho_{\mathscr{R}}\lambda_{g_2}}\right),$$

$$\Upsilon_{U_2}^{U_1,\text{hd,pro}} \triangleq \frac{\Gamma\left(m_{h_1}, \omega_2^{\text{pro}}\gamma_{\text{th},U_2}^{\text{hd}}\sigma_{U_1}^{\text{hd,pro}}\right)}{\Gamma\left(m_{g_1}\right)\Gamma\left(m_{h_1}\right)} \cdot \Gamma\left(m_{g_1}, \frac{m_{g_1}\gamma_{th,U_2}^{\text{hd}}\sigma_{U_2}^{U_1,\text{hd,pro}}}{\rho_{\mathscr{R}}^{\text{pro}}\lambda_{g_1}}\right). \tag{44}$$

Proof 5. It can be achieved by using the similar analysis that in the FD mode.

5. Numerical Results

In this section, the effectiveness channel factor to the NOMA relaying system is simulated. In the simulation, the noise is normalized, i.e., $N_0 = 1$. The final results are averaged over 10^6 realization runs. For fairness in comparison, we assume the total power budget to equal ρ, the transmitted power is set up for conventional cooperative NOMA scheme $\rho_B = \rho_{\mathscr{R}} \triangleq \rho/2$ and that for the user-aided relaying scheme $\rho_B = \rho_{\mathscr{R}} = \rho_{U_1} \triangleq \rho/3$. Unless other stated, the target rates of U_1 and U_2 are set $R_1 = 0.5$ and $R_2 = 1$, respectively. The allocated power fraction be $a_1 = 0.2$ so that $a_2 = 0.8$. We also set the fading severity parameter as $m_{h_1} = m_{h_r} = m_{g_2} = m_{f_r} = m_{f_1} \triangleq m$.

The system model is conducted as Figure 2. The distances between nodes x and y are denoted d_{xy} with $(x, y) \in \{(b, r), (r, 2), (b, 1), (r, 1), (1, 2)\}$. We normalize $d_{br} = d_{r2} = 1$ and $d_{b1} = 0.7$. The angle between $B \longrightarrow \mathscr{R}$ link and $B \longrightarrow U_1$ link is α. Hence, the space form relay to U_1 is $d_{r1}^2 = d_{br}^2 + d_{b1}^2 - 2d_{br}d_{b1}\cos(\alpha)$ and distance between U_1 and U_2 is $d_{12}^2 = (d_{br} + d_{r2})^2 + d_{b1}^2 - 2(d_{br} + d_{r2})d_{b1}\cos(\alpha)$. In order to invoke large-scale fading, the channel power mean parameters are set as the following function of distance, such as $\lambda_{h_1} = (1 - \kappa)d_{b1}^{-n}$, $\lambda_{h_2} = (1 - \kappa)d_{br}^{-n}$, $\lambda_{g_1} = (1 - \kappa)d_{12}^{-n}$, and $\lambda_{g_2} = (1 - \kappa)d_{r2}^{-n}$. $\lambda_{f_1} = \lambda_{f_2} = \varepsilon(1 - \kappa)d_{r1}^{-n}$. The power mean of self-interference links at relay and U_1 after precancellation is set $\lambda_{f_r} = \lambda_{f_{U_1}} = \varepsilon$, where κ is the imperfect CSI level, n is the exponential loss factor, and ε represents the interference mitigation level. Unless other stated, we set $\alpha = \pi/4$, $n = 3$, and $\varepsilon = 0.01$.

Figures 3 and 4 plot the impact of the fading parameter m on the outage performance with varying total transmitted power. It is experimentally illustrated that the fading parameters of the transmission links have a great influence on the outage performance. The outage performance with a higher m outperforms the ones with the lower m. This is because a higher m implies a stronger received SNR at destination. Furthermore, the main reason is that a larger fading parameter leads to a higher diversity order for the user, resulting in a lower outage probability [18]. As shown in Figures 3 and 4, analysis results match very well with the Monte Carlo simulation curves.

Performance gap can be seen among three cases of outage probability related to users U_1 and U_2. Furthermore, there exists a saturation for the outage probability in the higher transmit power region. One can also observe from Figure 4 that the fading parameters of all links ($m = 5$) have crucial impact on the outage performance.

Figures 5 and 6 investigate the impact of imperfect CSI level on the outage performance of the system.

Figure 7 provides a comparison of the achievable throughput by considering two concerned modes at relay. Note that the considered system also gains benefit of the FD scheme and achieves a higher throughput as increasing the fading parameters. However, performance gap as varying fading parameters can be seen clearly in transmitting power ranging from 10 dB to 20 dB for the FD scheme and ranging from 15 dB to 25 dB for the HD scheme. It is worth noting

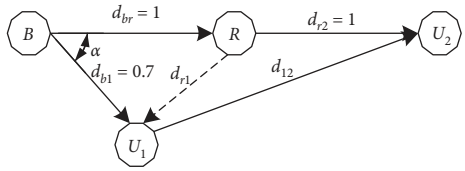

FIGURE 2: The setup system model.

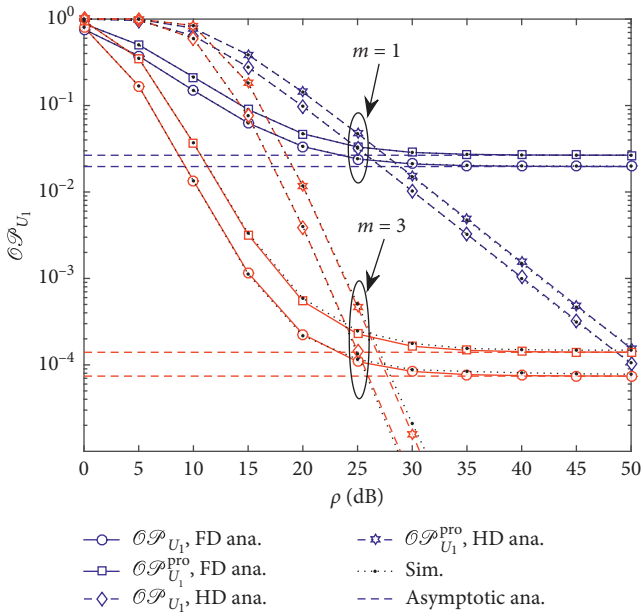

FIGURE 3: The outage probability of U_1 under impact of fading severity factor m with perfect CSI, i.e., $\kappa = 0$.

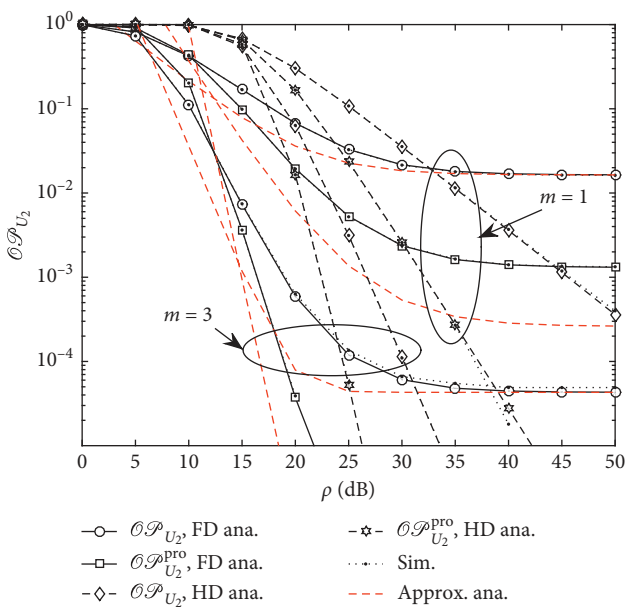

FIGURE 4: The outage probability of U_2 under impact of fading severity factor m with perfect CSI, i.e., $\kappa = 0$.

that throughput performance of the HD scheme for the one time slot is lower than the remaining schemes. To sum up, the better channel condition leads to higher throughput can

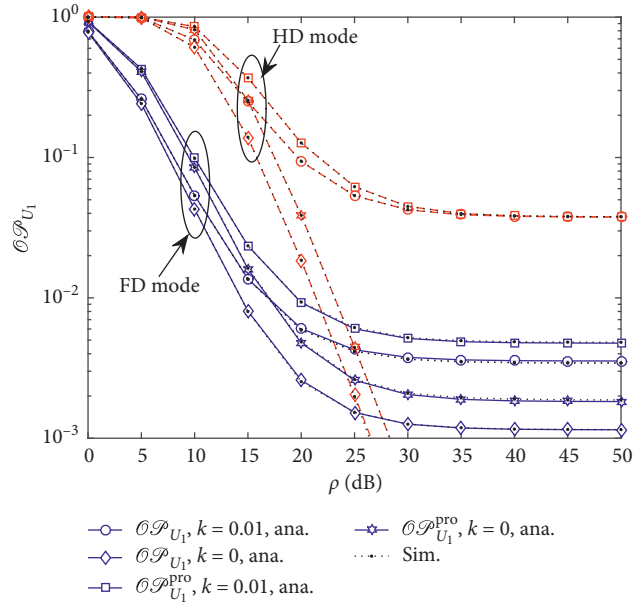

FIGURE 5: The outage probability of U_2 under impact of imperfect CSI level κ with fading severity factor $m = 2$.

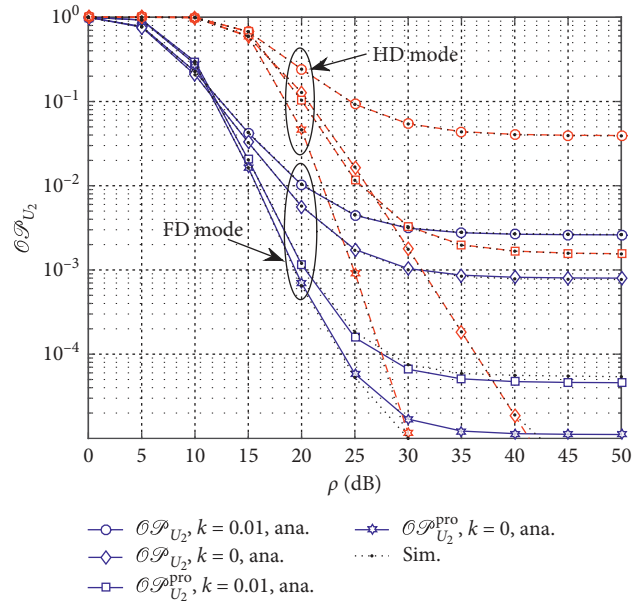

FIGURE 6: The outage probability of U_2 under impact of imperfect CSI level κ with fading severity factor $m = 2$.

be obtained and such throughput reaches the limited value at a high level of transmitting power at B. Such observations verify the accuracy of our derived expressions.

From Figure 8, we can see that the NOMA using the FD mode always outperforms the NOMA using the HD mode in terms of the optimal energy efficiency. Interestingly, optimal energy efficiency can be achieved at the FD mode and HD mode during the first time slot, but such values can only be found by using the numerical method. Moreover, the low energy efficiency can be seen at high transmitting power of B.

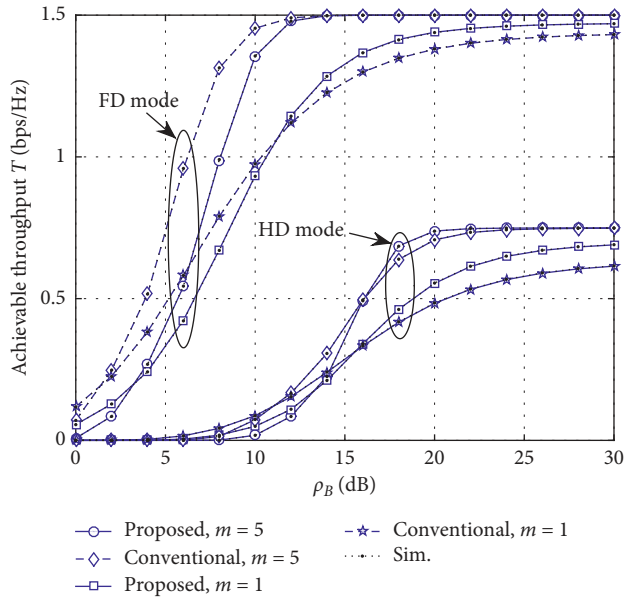

FIGURE 7: The sum throughput of the NOMA relaying network over Nakagami-m fading, for different values of $m = [1, 5]$ with $\kappa = 0.01$.

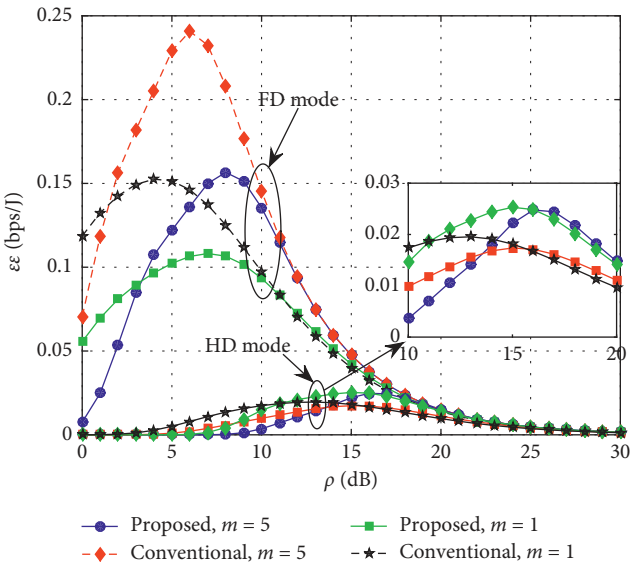

FIGURE 8: The energy efficiency of the NOMA relaying network over Nakagami-m fading, for different values of $m = [1, 5]$.

The reason is that putting more power at B reduces energy efficiency of the considered system.

Figures 9 and 10 show the variation of outage performance of U_1 and U_2 under impact of angle α with $\kappa = 0.01$, $m = 3$, and $\varepsilon = 0.1$. As can be seen from Figure 9, the outage probability of FD network decreases when α increases from 0 to π. This is due to the decline of interference from relay to U_1 since the distance between these nodes grow. However, performance of the HD scheme does not suffer from this variation. From Figure 10, there are some fluctuations of U_2 outage. Outage performance of the proposed user-aided relaying FD scheme outperforms than that of the conventional scheme when $\alpha \geq \pi/4$. This can be explained that since

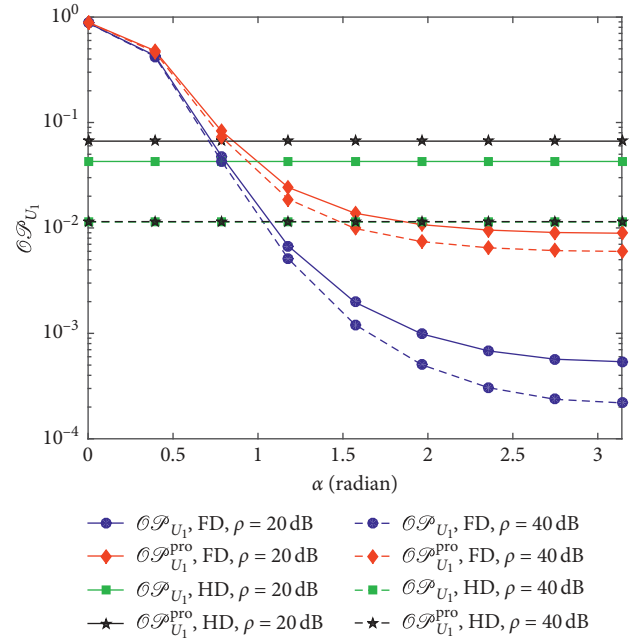

FIGURE 9: The U_1 outage probability versus angle $\alpha = [0, \pi]$, for different values of $\rho = [20, 40]$dB.

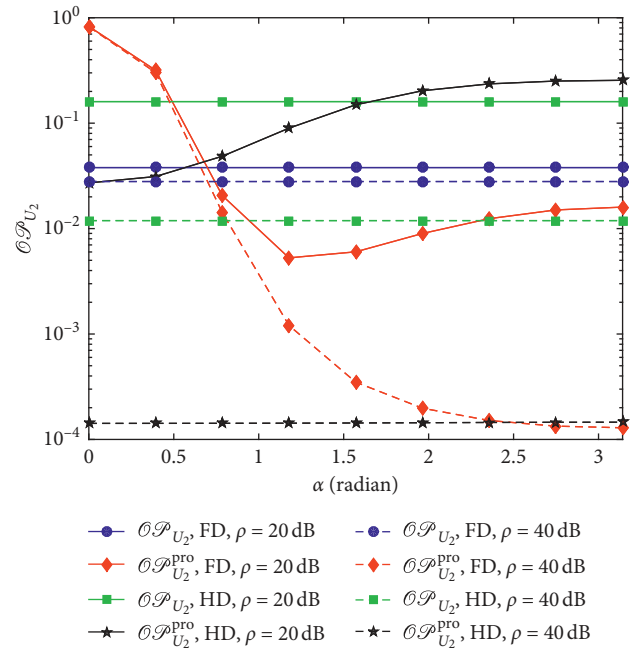

FIGURE 10: The U_1 outage probability versus angle $\alpha = [0, \pi]$, for different values of $\rho = [20, 40]$dB.

space between relay and user U_1 is large enough, it leads to the small interference between nodes and improves the proposed user-aided relying.

6. Conclusion

In this paper, the system performance of cooperative NOMA networks over imperfect Nakagami-m fading environments

has been studied. We have derived the closed-form expressions of the outage probability and delay-limited throughput and energy efficiency for both conventional relaying and near user-aided relaying for the cooperative NOMA system. The numerical simulations have been conduced to verify the exactness of analytical expressions. The results show that the system performance can further be enhanced by improving either severity parameter m or exactness of the channel as imperfect CSI is raised. In addition, the simulation results also reveal that the near user-based relaying for the cooperative NOMA scheme can improve far user performance; however, it degrades that of near user.

Appendix

Substituting (6) and (7) into (19), the U_1 outage probability can be simplified after some simple manipulations as

$$\begin{aligned}\mathcal{OP}_{U_1} &= 1 - \Pr\left\{\gamma_{U_2,U_1} \geq \gamma_{\text{th},U_2}, \gamma_{U_1,U_1} \geq \gamma_{\text{th},U_1}\right\} \\ &= 1 - \Pr\left\{\rho_B \vartheta \left|h_1\right|^2 \geq \rho_{\mathcal{R}} \left|f_1\right|^2 + \sigma_{U_1}\right\},\end{aligned} \tag{A.1}$$

where ϑ is defined in Proposition 1. To tackle (A.1), we consider two scenarios as below.

Case 1. In the case $\vartheta \leq 0$, i.e., $\gamma_{\text{th},U_2} > a_2/a_1$, the outage probability is always equal to one, i.e., $\mathcal{OP}_{U_1} = 1$.

Case 2. In the case $\vartheta > 0$, i.e., $\gamma_{\text{th},\mathcal{U}_2} \leq a_2/a_1$, (A.1) can be computed as

$$\mathcal{OP}_{U_1} = 1 - \int_0^{\infty} \left(1 - F_{|h_1|^2}\left(\frac{\rho_{\mathcal{R}} x + \sigma_{U_1}}{\rho_B \vartheta}\right)\right) f_{|f_1|^2}(x)\, dx. \tag{A.2}$$

According to (2) and (3), (A.2) can be solved as

$$\begin{aligned}\mathcal{OP}_{U_1} &= 1 - \psi \sum_{i=0}^{m_{h_1}-1} \omega^i \int_0^{\infty} x^{m_{f_1}-1} e^{-\Omega x} \frac{\left(\rho_{\mathcal{R}} x + \sigma_{U_1}\right)^i}{i!} dx \\ &\overset{(a)}{=} 1 - \psi \sum_{i=0}^{m_{h_1}-1} \sum_{k=0}^{i} \binom{i}{k} \frac{\omega^i \sigma_{U_1}^{i-k} \rho_{\mathcal{R}}^k}{i!} \int_0^{\infty} x^{k+m_{f_1}-1} e^{-\Omega x}\, dx \\ &\overset{(b)}{=} 1 - \psi \sum_{i=0}^{m_{h_1}-1} \sum_{k=0}^{i} \binom{i}{k} \frac{\omega^i \sigma_{U_1}^{i-k} \rho_{\mathcal{R}}^k \Gamma\left(k + m_{f_1}\right)}{i! \Omega^{k+m_{f_1}}},\end{aligned} \tag{A.3}$$

where ω, Ω, and ψ are defined in (20). Step (a) applies in Eq. 1.111 of [34] and step (b) uses equality in Eq. 3.381.4 of [34] . Combining the above two cases, Proposition 1 is derived, and this is the end of perfect explanation for such proposition.

Since $\gamma_{U_2,\mathcal{R}}$ and γ_{U_2,U_2} are independent to each other, $\mathcal{OP}_{U_2}$ in (29) can be further simplified as

$$\mathcal{OP}_{U_2} = 1 - \underbrace{\Pr\left\{\gamma_{U_2,\mathcal{R}} \geq \gamma_{\text{th},U_2}\right\}}_{\mathcal{OP}_{U_2,1}} \times \underbrace{\Pr\left\{\gamma_{U_2,U_2} \geq \gamma_{\text{th},U_2}\right\}}_{\mathcal{OP}_{U_2,2}}. \tag{A.4}$$

The $\mathcal{OP}_{U_2,1}$ item can be revealed as the same as in (A.3) and given by

$$\mathcal{OP}_{U_2,1} = \begin{cases} 0, & \vartheta_2 \leq 0, \\ \psi_2 \sum_{i=0}^{m_{h_2}-1} \sum_{k=0}^{i} \binom{i}{k} \frac{\omega_2^i \sigma_{\mathcal{R}}^{i-k} \rho_{\mathcal{R}}^k \Gamma\left(k + m_{f_r}\right)}{i! \Omega_2^{k+m_{f_r}}}, & \vartheta_2 > 0. \end{cases} \tag{A.5}$$

In addition, the second item, i.e., $\mathcal{OP}_{U_2,2}$, can be calculated as follows:

$$\begin{aligned}\mathcal{OP}_{U_2,2} &= \Pr\left\{\frac{\rho_{\mathcal{R}} \left|g_2\right|^2}{\sigma_{U_2}} \geq \gamma_{\text{th},U_2}\right\} \\ &= \frac{1}{\Gamma\left(m_{g_2}\right)} \Gamma\left(m_{g_2}, \frac{m_{g_2} \sigma_{U_2} \gamma_{\text{th},U_2}}{\rho_{\mathcal{R}} \lambda_{g_2}}\right).\end{aligned} \tag{A.6}$$

Finally, substituting every computed equation into main formula, Proposition 3 is derived. This is the end of the proof.

Data Availability

No data were used to support this study.

Conflicts of Interest

The authors declare that they have no conflicts of interest.

References

[1] D. Wan, M. Wen, F. Ji, H. Yu, and F. Chen, "Non-orthogonal multiple access for cooperative communications: challenges, opportunities, and trends," *IEEE Wireless Communications*, vol. 25, no. 2, pp. 109–117, 2018.

[2] L. Dai, B. Wang, Z. Ding, Z. Wang, S. Chen, and L. Hanzo, "A survey of non-orthogonal multiple access for 5G," *IEEE Communications Surveys & Tutorials*, vol. 20, no. 3, pp. 2294–2323, 2018.

[3] Z. Ding, Y. Liu, J. Choi et al., "Application of non-orthogonal multiple access in LTE and 5G networks," *IEEE Communications Magazine*, vol. 55, no. 2, pp. 185–191, 2017.

[4] D. T. Do and H. S. Nguyen, "A tractable approach to analyze the energy-aware two-way relaying networks in presence of co-channel interference," *EURASIP Journal on Wireless Communications and Networking*, vol. 2016, no. 1, p. 271, 2016.

[5] D. T. Do, H. S. Nguyen, M. Voznak, and T. S. Nguyen, "Wireless powered relaying networks under imperfect channel state information: system performance and optimal policy for instantaneous rate," *Radioengineering*, vol. 26, no. 3, pp. 869–877, 2017.

[6] X. X. Nguyen and D. T. Do, "Maximum harvested energy policy in full-duplex relaying networks with SWIPT"," *International Journal of Communication Systems*, vol. 30, no. 17, article e3359, 2017.

[7] C. Zhong, H. A. Suraweera, G. Zheng, I. Krikidis, and Z. Zhang, "Wireless information and power transfer with full duplex relaying," *IEEE Transactions on Communications*, vol. 62, no. 10, pp. 3447–3461, 2014.

[8] T. L. Nguyen and D. T. Do, "A new look at AF two-way relaying networks: energy harvesting architecture and impact of co-channel interference"," *Annals of Telecommunications*, vol. 72, no. 11-12, pp. 669–678, 2017.

[9] C. Zhong and Z. Zhang, "Non-orthogonal multiple access with cooperative full-duplex relaying," *IEEE Communications Letters*, vol. 20, no. 12, pp. 2478–2481, 2016.

[10] X. Yue, Y. Liu, S. Kang, A. Nallanathan, and Z. Ding, "Exploiting full/half-duplex user relaying in NOMA systems," *IEEE Transactions on Communications*, vol. 66, no. 2, pp. 560–575, 2018.

[11] T. L. Nguyen and D. T. Do, "Exploiting impacts of intercell interference on SWIPT-assisted non-orthogonal multiple access," *Wireless Communications and Mobile Computing*, vol. 2018, article 2525492, 12 pages, 2018.

[12] L. Lv, Q. Ni, Z. Ding, and J. Chen, "Application of non-orthogonal multiple access in cooperative spectrum-sharing networks over Nakagami-*m* fading channels," *IEEE Transactions on Vehicular Technology*, vol. 66, no. 6, pp. 5506–5511, 2017.

[13] L. Lv, J. Chen, and Q. Ni, "Cooperative non-orthogonal multiple access in cognitive radio," *IEEE Communications Letters*, vol. 20, no. 10, pp. 2059–2062, 2016.

[14] J. B. Kim and I. H. Lee, "Capacity analysis of cooperative relaying systems using non-orthogonal multiple access," *IEEE Communications Letters*, vol. 19, no. 11, pp. 1949–1952, 2015.

[15] M. Xu, F. Ji, M. Wen, and W. Duan, "Novel receiver design for the cooperative relaying system with non-orthogonal multiple access," *IEEE Communications Letters*, vol. 20, no. 8, pp. 1679–1682, 2016.

[16] J. B. Kim and I. H. Lee, "Non-orthogonal multiple access in coordinated direct and relay transmission," *IEEE Communications Letters*, vol. 19, no. 11, pp. 2037–2040, 2015.

[17] T. M. C. Chu and H. J. Zepernick, "Performance of a non-orthogonal multiple access system with full-duplex relaying," *IEEE Communications Letters*, vol. 22, no. 10, pp. 2084–2087, 2018.

[18] J. Men, J. Ge, and C. Zhang, "Performance analysis of non-orthogonal multiple access for relaying networks over Nakagami-*m* fading channels," *IEEE Transactions on Vehicular Technology*, vol. 66, no. 2, pp. 1200–1208, 2017.

[19] X. Yue, Y. Liu, S. Kang, and A. Nallanathan, "Performance analysis of NOMA with fixed gain relaying over Nakagami-*m* fading channels," *IEEE Access*, vol. 5, pp. 5445–5454, 2017.

[20] H. S. Nguyen, A. H. Bui, D. T. Do, and M. Voznak, "Imperfect channel state information of AF and DF energy harvesting cooperative networks," *China Communications*, vol. 13, no. 10, pp. 11–19, 2016.

[21] Z. Yang, Z. Ding, P. Fan, and N. Al-Dhahir, "The impact of power allocation on cooperative non-orthogonal multiple access networks with SWIPT," *IEEE Transactions on Wireless Communications*, vol. 16, no. 7, pp. 4332–4343, 2017.

[22] X. X. Nguyen and D. T. Do, "Optimal power allocation and throughput performance of full-duplex DF relaying networks with wireless power transfer-aware channel," *EURASIP Journal on Wireless Communications and Networking*, vol. 2017, no. 1, p. 152, 2017.

[23] Z. Ding, P. Fan, and H. V. Poor, "On the coexistence between full-duplex and NOMA," *IEEE Wireless Communications Letters*, vol. 7, no. 5, pp. 692–695, 2018.

[24] M. B. Shahab and S. Y. Shin, "Time shared half/full-duplex cooperative NOMA with clustered cell edge users," *IEEE Communications Letters*, vol. 22, no. 9, pp. 1794–1797, 2018.

[25] Z. Xiao, Y. Li, L. Bai, and J. Choi, "Achievable sum rates of half- and full-duplex bidirectional OFDM communication links," *IEEE Transactions on Vehicular Technology*, vol. 66, no. 2, pp. 1351–1364, 2017.

[26] Y. Sun, D. W. K. Ng, Z. Ding, and R. Schober, "Optimal joint power and subcarrier allocation for full-duplex multicarrier non-orthogonal multiple access systems," *IEEE Transactions on Communications*, vol. 65, no. 3, pp. 1077–1091, 2017.

[27] D. Wan, M. Wen, H. Yu, Y. Liu, F. Ji, and F. Chen, "Non-orthogonal multiple access for dual-hop decode-and-forward relaying," in *Proceedings of 2016 IEEE Global Communications Conference (GLOBECOM)*, pp. 1–6, Washington, DC, USA, December 2016.

[28] J. Men and J. Ge, "Non-orthogonal multiple access for multiple antenna relaying networks," *IEEE Communications Letters*, vol. 19, no. 10, pp. 1686–1689, 2015.

[29] C. Xue, Q. Zhang, Q. Li, and J. Qin, "Joint power allocation and relay beamforming in non-orthogonal multiple access amplify-and-forward relay networks," *IEEE Transactions on Vehicular Technology*, vol. 66, no. 8, pp. 7558–7562, 2017.

[30] D. Wan, M. Wen, F. Ji, Y. Liu, and Y. Huang, "Cooperative NOMA systems with partial channel state information over Nakagami-*m* fading channels," *IEEE Transactions on Communications*, vol. 66, no. 3, pp. 947–958, 2018.

[31] H. A. Suraweera, I. Krikidis, G. Zheng, C. Yuen, and P. J. Smith, "Low-complexity end-to-end performance optimization in MIMO full-duplex relay systems," *IEEE Transactions on Wireless Communications*, vol. 13, no. 2, pp. 913–927, 2014.

[32] D. Choi and J. H. Lee, "Outage probability of two-way full-duplex relaying with imperfect channel state information," *IEEE Communications Letters*, vol. 18, no. 6, pp. 933–936, 2014.

[33] J. Men, J. Ge, and C. Zhang, "Performance analysis for downlink relaying aided non-orthogonal multiple access networks with imperfect CSI over Nakagami-fading," *IEEE Access*, vol. 5, pp. 998–1004, 2017.

[34] I. S. Gradshteyn and I. M. Ryzhik, *Table of Integrals, Series, and Products*, Academic Press, Inc., Cambridge, MA, USA, 7th edition, 2007.